Ecological Modelling 508 (2025) 111212

Contents lists available at ScienceDirect

Ecological Modelling

journal homepage: www.elsevier.com/locate/ecolmodel

HuHoLa: A novel Hummock-Hollow-Lawn mire microtopography modelling approach

Koffi Dodji Noumonvi [a,*], Nils Helge Havertz [a,b], Jonas Bohlin [c], Sebastian van der Linden [d], Mats B. Nilsson [a], Matthias Peichl [a]

[a] Department of Forest Ecology and Management, Swedish University of Agricultural Sciences, 90183 Umeå, Sweden
[b] Institute of Botany and Landscape Ecology, University of Greifswald – Partner in the Greifswald Mire Centre, 17489 Greifswald, Germany
[c] Department of Forest Resource Management, Swedish University of Agricultural Sciences, 90183 Umeå, Sweden
[d] Institute of Geography and Geology, University of Greifswald – Partner in the Greifswald Mire Centre, 17489 Greifswald, Germany

ARTICLE INFO

Keywords:
Peatland microtopography modelling
Digital elevation model
Hummocks
Hollows, Lawns

ABSTRACT

Peatlands play a crucial role in global carbon storage and methane emissions. Microtopographic features (hummocks, hollows, and lawns) are one of their main characteristics. These features strongly influence hydrological and biogeochemical processes, affecting vegetation patterns and greenhouse gas exchanges. Traditional methods for mapping peatland microtopography often rely on complex algorithms or require extensive field data, typically producing only a binary hummock-hollow classification. These shortcomings limit their applicability for large-scale studies. To address these challenges, we developed and validated HuHoLa (Hummock-Hollow-Lawn), an easy applicable and scalable model that classifies peatland microtopography using only a digital elevation model (DEM). HuHoLa applies a sink-filling approach to generate classifications, with a key feature being a threshold value to better capture the subtle variations in the non-flat lawn features. In addition to the microtopographic classification, the model provides a secondary output that acts as a proxy for water table depth (WTD) and soil temperature (Ts), thus offering a useful tool for understanding spatial variations in WTD and Ts across peatland landscapes. HuHoLa delivers a more nuanced and realistic depiction of peatland surface structure compared to traditional binary methods, with field-based validation demonstrating robust performance (Kappa coefficients of 0.62 and 0.81 for DEM resolutions of 30 cm and 50 cm, respectively) that outperforms traditional binary classification approaches (Kappa $<$ 0.5 for DEM resolutions between 10 and 25 cm). The model is particularly suited for large-scale research applications. Its simplicity, requiring only a DEM, combined with its multi-purpose use, makes it an effective tool for advancing peatland studies and integrating with land surface models.

1. Introduction

Boreal peatlands play a pivotal role in the global carbon (C) cycles, acting as a long-term C sink and a source of atmospheric methane (Frolking et al., 2011). The biogeochemical mechanisms behind the peatland C dynamics are complex, and the fate of the stored C is uncertain under the ongoing climate change, as different scenarios suggest a shift from sink to source in the coming decades (Wu and Blodau, 2013; Zhao and Zhuang, 2023). Among the several factors that influence biogeochemical processes in peatlands, microtopography emerges as an important factor with a strong influence on peatland C fluxes (Moore and Knowles, 1989). Despite the known importance of microtopography in peatland processes, land surface models used for simulating and prognosing carbon dynamics have long overlooked this importance of microtopography in their processes, though some recent studies suggested improvements in model accuracy when accounting for microtopography (Graham et al., 2022).

Microtopography consists of small scale variations of the uppermost peat layer typically spanning from several centimetres to a few meters, created and sustained by environmental gradients (particularly water table depth, WTD), differential plant growth and peat accumulation (Nilsson, 2002). These features are often broadly classified into hummocks, hollows, and lawns depending on their position relative to the average WTD (Belyea and Baird, 2006; Nungesser, 2003). While

* Corresponding author.
E-mail address: koffi.noumonvi@slu.se (K.D. Noumonvi).

https://doi.org/10.1016/j.ecolmodel.2025.111212
Received 30 January 2025; Received in revised form 15 May 2025; Accepted 31 May 2025
Available online 12 June 2025

hummocks are locally elevated and drier areas with elevations of 20 - 50 cm over the mean water table, hollows are often described as lower flatter areas or shallow depressions with close proximity to the water table and are frequently fully inundated (Belyea and Baird, 2006; Nungesser, 2003; Pouliot et al., 2011). Intermediary between hummocks and hollows are lawns, often the most represented microform, forming larger and relatively flat surfaces with elevations of 5 - 20 cm over the average water table (Rydin and Jeglum, 2006). In northern aapa mire fens, boreal mixed mires and raised bogs, special elongated mosaic patterns can occur when gentle slopes prevail along with the cold climate (Laitinen et al., 2005). Elongated hummocky structures are called strings, functioning as damming ridges, and are usually alternated with deeper wetter areas called flarks. Those mosaic features are often 5-20 m long and can be some meters wide (Joosten and Clarke, 2002; Rydin and Jeglum, 2013).

Several approaches have been suggested over time for mapping peatland surface microtopography. Early modelling attempts to model peatland microtopography were mostly processbased models that relied on the conceptual understanding of the genesis and maintenance of microforms (Nungesser, 2003). The complexity of such process-based models, and their requirement of multiple inputs limited their applicability over entire mires. With the recent advances in remote sensing technologies, different models emerged, allowing to model microtopography at finer spatial resolutions (down to 1 cm). These models make use of data from different remote sensing techniques such as terrestrial laser scanning (Graham et al., 2020, 2022; Stovall et al., 2019), airborne laser scanning (Brubaker et al., 2013; Kalacska et al., 2021; Korpela et al., 2020), or Structure from motion (SfM) based on unmanned aerial vehicle (UAV) images (Kalacska et al., 2021; Korpela et al., 2020; Lovitt et al., 2017; Moore et al., 2019). These techniques can broadly be grouped into machine learning algorithms (Kalacska et al., 2021; Korpela et al., 2020), hydrological and catchment delineation algorithms (Brubaker et al., 2013; Stovall et al., 2019) or elevation distribution and threshold approaches (Graham et al., 2020, 2022; Lovitt et al., 2017; Moore et al., 2019). While machine learning based methods require intensive field data as training features, several of the other methods were tested at a plot scale, and their large-scale applicability is not guaranteed. Furthermore, except Korpela et al. (2020) who used a machine learning approach to classify microtopography into multiple classes, all other approaches produce a binary hummock-hollow output, thus not isolating the intermediate most represented lawn class in most peatlands. Thus, there is a need for simple models based on easily available input data that are robust at the landscape scale and able to distinguish multiple microtopography classes.

WTD and soil temperature (Ts) are critical factors influencing peatland biogeochemistry, as they jointly regulate microbial activity, plant growth, and nutrient cycling (Moore and Knowles, 1989; Page and Baird, 2016). Fluctuations in WTD can create varying anaerobic conditions, significantly affecting carbon storage and greenhouse gas emissions, while Ts influences microbial metabolism and decomposition rates (Page and Baird, 2016; Sirin, 2023). Traditional methods for measuring these parameters often rely on point measurements, which may not capture the full spatial variability across peatland landscapes. This highlights the need for innovative approaches capable of spatially distributed mapping of both WTD and Ts. Given that microtopography is closely linked to WTD and influences spatial variations in Ts, these models can also provide valuable insights for modelling spatially WTD and Ts in peatlands.

To fill these gaps, this study proposes a novel hydrological method (HuHoLa for Hummock-Hollow-Lawn) for classifying peatland microtopography over entire mires, based on a digital elevation model (DEM), with a secondary Ts and WTD proxy output. The main objectives of this study were to: (1) present the algorithm of the HuHoLa model as well as its inputs and outputs, (2) assess its performance and applicability at different spatial resolutions of DEM and (3) test the potential of using the depth and height of hollows and hummocks as a proxy for Ts and WTD.

2. Materials and methods

2.1. Study site and data acquisition

The development and testing of the HuHoLa model used data from the Kulbäcksliden research infrastructure (KRI), located near the municipality of Vindeln in Northern Sweden (Fig. 1). The KRI includes a mire complex with four sites (Degerö Stormyr, Stortjärn, Hålmyran and Hälsingfors Stormyran), with intensive peatland research ongoing since 1995. The vegetation of the study area is dominated by Sphagnum mosses and sedges, with scattered dwarf shrubs (e.g., *Andromeda polifolia, Calluna vulgaris*, …) occurring on some hummocks (Noumonvi et al., 2023).

The digital elevation models (DEMs) used to develop the HuHoLa model were produced from LiDAR data collected in September 2019 with a Riegl VQ-1560i- DW (dual wave 532 nm and 1064 nm) airborne laser scanner with a density of 20 points.m^{-2} per channel (Noumonvi et al., 2023). The LiDAR data was used to produce 30 × 30 cm and 50 × 50 cm resolution DEMs. Additionally, we made use of SfM to produce finer scale resolution DEMs (3 × 3 cm), based on UAV images collected in September 2023 (between 10 am and 2 pm) by a DJI Phantom 4 UAV equipped with a five band multispectral camera (Blue: 450 nm ± 16 nm, Green: 560 nm ± 16 nm, Red: 650 nm ± 16 nm, Red Edge: 730 nm ± 16 nm, and Near-InfraRed: 840 nm ± 26 nm). Furthermore, the UAV-based DEM was resampled down to 6, 10, 20, 30, 40, 50, 60, 70, 80, 90 and 100 cm resolution for a sensitivity analysis.

Validation field data for the microtopography classification were collected at the Degerö Stormyr site, selected for its large size (271 ha) and its representation of all mire microforms. The site also features an extensive network of boardwalks, making it ideal for data collection. A total of 260 reference points were collected to validate the HuHoLa microtopography classes, with each point positioned 2 m from the boardwalk using high-precision RTK-GNSS (Fig. 1c).

Time-series data for Ts, measured with HOBO MX2303 loggers, and manual WTD measurements were gathered from four distinct microtopographic locations at each of three other sites (Stortjärn, Hälsingfors Stormyran, and Hålmyran) along with Degerö Stormyr. The average Ts and WTD data were then correlated with the secondary "depth and height of hollows and hummocks" output from the HuHoLa model.

2.2. HuHoLa model

The inputs, workflow and outputs of the HuHoLa algorithm are presented in Fig. 2, and its Python implementation is available at https://github.com/bravemaster3/huhola.

2.2.1. Model input

The HuHoLa model requires two inputs: a DEM, and a classification threshold to be applied on one of the intermediary outputs. Given that microforms vary in size, the resolution of the DEM would play an important role in the size of microforms that can be detected by the model. This does not necessarily mean however that the finer resolution, the better, due to the underlying functioning of the model which is mainly based on filling sinks. The classification threshold depends highly on the DEM, since the DEM will be more contrasted, i.e. with more surface roughness, in higher resolution DEMs. This means that without considering a threshold (i.e. threshold = 0), the model will result in a more fragmented microtopography, with any small change in elevation leading potentially to a hummock and hollow, although lawns are not completely flat in reality. Through systematic sensitivity analysis across different DEM resolutions (more details in Section 2.4), we empirically determined optimal threshold values.

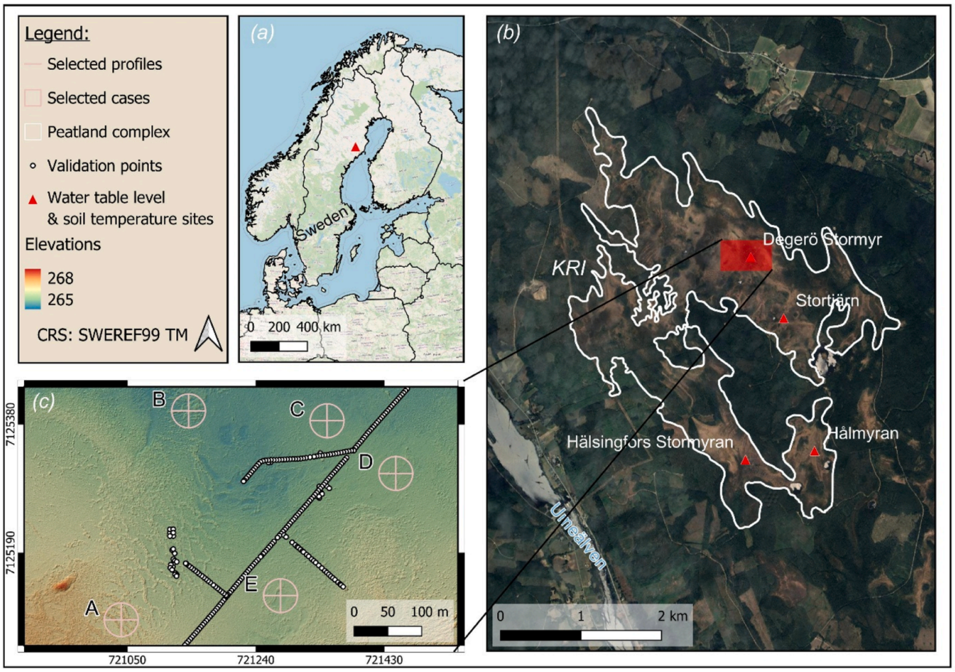

Fig. 1. Data collection sites. (a) Location in northern Sweden shown by the red triangle. (b) Google satellite background with the extents of the peatland complex where the data was collected, and red triangles represent the four sites (Degerö Stormyr, Stortjärn, Hålmyran, and Hälsingfors Stormyran) where manual water table measurement and Ts data were collected. (c) digital elevation model showing elevations above sea level across a part of the Degerö Stormyr site, with the dots representing the 260 validation points collected along a boardwalk, two meters away, the circles and cross horizontal/vertical lines representing selected cases and profiles for showing a close view of the mapped topography with elevations.

2.2.2. Model outputs

There are two intermediary outputs of the HuHoLa algorithm: the filled DEM (FillDEM) and the filled inverted DEM (FillInvDEM), which can also to some extent be considered as the hollow fill depth and the hummock fill depth, respectively. There is another output that is intermediary when HuHoLa is used to classify microtopography, but is also the final output when HuHoLa is used to create a WTD proxy: the hollow-hummock-depth-height (HHDH). The microtopography outputs consist of a three-class or a five-class microtopography raster layer.

2.2.3. Algorithm description

The key workflow steps of the HuHoLa model can be summarized as follows (Fig. 2):

Step 1: Filling depressions in the DEM

While depression filling algorithms are commonly used in hydrological applications such as catchment delineation to eliminate depressions and create hydrologically consistent surfaces for flow modelling (Jenson and Domingue, 1988), HuHoLa uses depression filling to identify microtopographic features by analysing the filled depths in the DEM. The DEM is filled using the “Fill Depressions” algorithm developed by Wang and Liu (2006). This algorithm is the default “Fill Depressions” method in HuHoLa, chosen for its efficiency for high resolution DEMs, although two other alternatives, the “Fill Depressions” algorithm by Planchon and Darboux (2002) and the classic “Fill Depressions” algorithm implemented in whitebox tools (Lindsay, 2016) can be used in HuHoLa. This step fills all depressions in the DEM, considered here as hollows. When HuHoLa is used to produce a WTD proxy, the “Fill Depressions” in this step (only in step 1) should apply a “fix flats”, an optional flag in the “Fill Depressions” tool (Lindsay, 2016) which allows to apply a small gradient effectively letting the fill to spill over and let the water flow through the peatland surface. On the other hand, no “fix flats” should be applied when classifying microtopography.

Step 2: Filling depressions in the inverted DEM

In this step, the DEM is inverted by subtracting the DEM from the maximum value of the DEM (or any other elevation value higher than the highest point of the area of interest (Eq. (1)). This operation effectively turns upside down the terrain, and hollows become hummocks and vice versa. All arithmetic operations in HuHoLa are pixel-wise raster arithmetics.

$$\text{Inverted DEM} = \text{DEM Max Value} - \text{DEM} \quad (1)$$

After the DEM inversion, the same “Fill Depressions” algorithm is applied as in step 1. No “fix flats” is applied here, neither for microtopography classification nor for WTD proxy generation.

Step 3: Subtracting the filled depth in the inverted DEM from the filled depth in the DEM

This step consists of subtracting the filled depth in the inverted DEM (FillInvDEM – InvDEM) from the filled depth in the DEM (FillDEM – DEM), producing a raster layer representing the filled depths of hollows and hummocks in the DEM and inverted DEM, respectively, in other words the hollow-hummock-depth-height (HHDH) layer (Eq. (2)). When a “fix flats” is applied in step 1, HHDH is the final output, and represents a WTD proxy that can be correlated to measured WTD at different location of the peatland to possibly produce a spatial WTD map. When instead HHDH is produced without applying a “fix flats” in step 1, it can be used as a proxy for Ts.

$$\textit{HHDH or WTD Proxy} = (\textit{FillDEM} - \textit{DEM}) - (\textit{FillInvDEM} - \textit{InvDEM}) \quad (2)$$

Step 4: Classification of the different microforms

For classifying HHDH (from step 3) into the three microforms (lawns, hollows and hummocks), a threshold dependent on the DEM resolution and provided as input to the model is used along with the following classification rules in a five classes output layer:

- **HHDH = 0, class 0 or lawns**: occurring when both of the filled depth in FillDEM and the filled depth in FillInvDEM are 0. Theoretically, this could also occur when they are different from 0 but

Fig. 2. Workflow of the HuHoLa model. Green rectangles represent the inputs of the model, blue rectangles represent intermediary outputs not used directly, red rectangles represent exported outputs, yellow diamonds represent operations performed in the model, and ellipses represent classification rules. Numbers represent the four sub-sections of the HuHoLa model: 1- filling the DEM, 2- filling the inverted DEM, 3- Subtracting the filled depth in the inverted DEM (FillInvDEM – InvDEM) from the filled depth in the DEM (FillDEM – DEM) to produce the hollow-hummock-depth-height or HHDH a.k.a. WTD proxy when "fix flats" is applied during subSection 1, 4- Classification into the different microforms. Classes 0, 1, 2, 3, and 4 in step 4 are respectively lawns, hollows, hummocks, lower level lawns, and upper level lawns.

have the same value. However, this does normally not occur for the same pixel.

- **HHDH > threshold, class 1 or hollows:** occurring when the filled depth in FillDEM is larger than the filled depth in FillInvDEM, and the difference is too large to be considered a lawn (i.e. (FillDEM – DEM) – (FillInvDEM – InvDEM) exceeds the positive threshold value).
- **HHDH < -threshold, class 2 or hummocks:** occurring when the filled depth in FillDEM is smaller than the filled depth in FillInvDEM, and the difference too large to be considered a lawn (i.e. (FillDEM – DEM) – (FillInvDEM – InvDEM) exceeds the negative threshold value).
- **0 < HHDH ≤ threshold, class 3 or lower level lawns**: occurring when the filled depth in FillDEM is larger than the filled depth in FillInvDEM, and the difference is not large enough to be considered a hollow (i.e. when (FillDEM – DEM) – (FillInvDEM – InvDEM) is positive but does not exceed the threshold value).

- **-threshold ≤ HHDH < 0, class 4 or upper level lawns**: occurring when the filled depth in FillDEM is smaller than the filled depth in FillInvDEM, and the difference is not large enough to be considered a hummock (i.e. when (FillDEM – DEM) – (FillInvDEM – InvDEM) is negative but does not exceed the negative threshold value).

The last two classes (3 and 4, i.e. lower and upper level lawns) are just conceptual, and were merged with class 0 (lawns), hence producing also a three classes output layer, which was the only field-validated microtopography output, since classes 3 and 4 were not differentiated from class 0 in the field.

In few cases where a "hummock" occurs in a depression (Fig. 3A) or a "depression" occurs on a hummock (Fig. 3B), corresponding pixels will be filled both in FillDEM and FillInvDEM. In such cases, if the height or depth of the ambiguous feature is greater than the depth or height of its surrounding microform, the ambiguous feature is classified as a different one (e.g. a hummock inside of a hollow, or a hollow inside a hummock). Otherwise, it is merged with its surrounding microform.

2.3. Validation

To assess the agreement between the model output and field observation, different accuracy metrics were computed such as the accuracy, precision, recall, F1-score and Kappa coefficient, all based on a confusion matrix.

Precision for a given class is the proportion of positive predictions for that class that were actually correct, i.e. the proportion of true positives (TP) by all positive, i.e. both true and false positives (TP and FP) identifications by the model for that class (Eq. (3)). A higher precision is synonymous to a lower commission error, indicating that the model is good at avoiding false positives.

$$Precision = \frac{TP}{TP + FP} \tag{3}$$

Recall for a given class is the ratio of correctly predicted positive observations to the total actual positive observations, i.e. both true positives and false negatives (FN) (Eq. (4)). A higher recall is synonymous to a lower omission error, indicating that the model is good at avoiding false negatives.

$$Recall = \frac{TP}{TP + FN} \tag{4}$$

There is a trade-off between precision and recall, i.e. improving one metric comes at the cost of the other (Hanczar and Nadif, 2019).

The F1 score combines precision and recall using their harmonic mean for a given class (Eq. (5)). It is particularly useful in situations where there is an uneven class distribution (class imbalance) and provides a balance between precision and recall.

$$F1\ score = \frac{2 * Precision * Recall}{Precision + Recall} \tag{5}$$

The previous three metrics are computed for individual classes, and can be the basis for several other metrics that provide a basis to evaluate the entire model instead of individual classes. While accuracy is a commonly used performance measure, representing the proportion of correct predictions made by the model (Eq. (6)), Cohen's Kappa statistic (Eq. (7)) can appear sometimes as a more robust alternative accounting for imbalanced occurrence of the different classes, and by comparing the model to a random classifier (Cohen, 1960; Sim and Wright, 2005).

$$Accuracy = \frac{TP + TN}{TP + TN + FP + FN} \tag{6}$$

$$Kappa = \frac{Po - Pe}{1 - Pe} \tag{7}$$

Where:

Po: is the observed proportion of agreement between the model's predictions and the true classes,

Pe: is the proportion of agreement expected by chance.

2.4. Sensitivity analysis of DEM resolution effects on the fill threshold

In order to identify the adequate threshold to be used as input of the HuHoLa model, areas considered to contain only one of the three classes (hummock, hollow, and lawn) were drawn visually, and the "Fill Depressions" algorithm was applied for the 30 cm and 50 cm resolution DEMs. The goal of this analysis is to understand the frequency distribution of fill depths for the different classes. Furthermore, the precision and recalls for each class were calculated, considering different fill thresholds for the HuHoLa classification (Fig. 2), and plotted together to determine the threshold that yields an equal error rate, i.e. where the precision and recall curves are both optimized.

Apart from the LiDARbased DEM, the UAV-based resampled DEMs were used to identify the threshold at which the highest Kappa coefficient occurs. For each DEM resolution (ranging from 3 cm to 1 m), we tested fill thresholds from 0 to 10 cm in 1 cm increments and calculated the Kappa coefficient for each combination. The threshold yielding the highest Kappa coefficient at each DEM resolution would be considered optimal for that resolution. All the previous analyses will provide insights regarding the choice of the threshold to be used in the HuHoLa model.

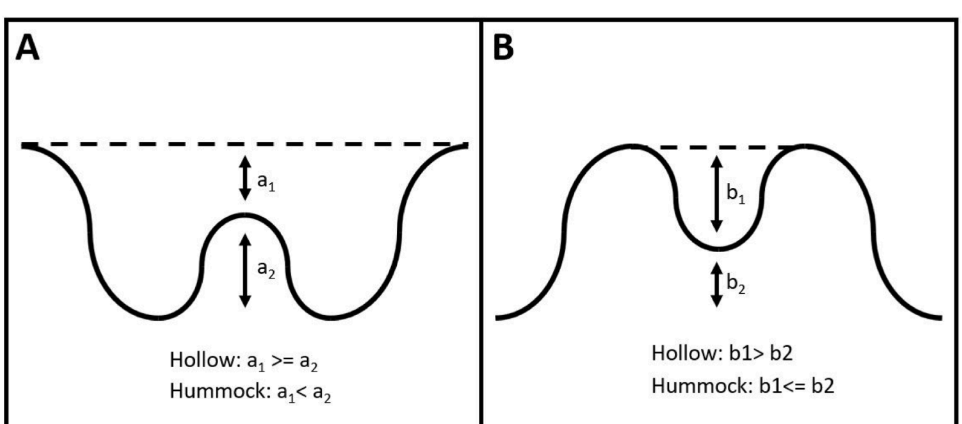

Fig. 3. Relative height difference and HuHoLa classification of (A) minor hummocky structures in hollows and (B) minor depressions on hummocks.

3. Results

3.1. Optimum DEM resolution and fill threshold

Our results show that lawns are never fully flat nor without elevation fluctuation, with some lawns having small positive (DEM) and negative (inverted DEM) fill values (up to ±4 or ±6 cm for 50 cm or 30 cm DEM respectively) (Fig. 4). The 99% percentiles of fill depth suggest a fill threshold of 5 to 6 cm for the 30 cm DEM, and 3 to 4 cm fill threshold for the 50 cm DEM. This suggests that pixels filled at less than this threshold are likely lawns, even though some edges of hummocks and hollows will also have these small fill depths. The fill depths for hollows are mostly positive while that of hummocks are mostly negative, i.e. hollows are not filled in the inverted DEM, whereas hummocks are not filled in the DEM.

The application of various thresholds in HuHoLa for classifying microtopography revealed a trade-off between precision and recall for different microtopography classes (hummocks, hollows, lawns) with increasing fill threshold (Fig. 5). Higher fill thresholds led to increased precision for lawns but decreased precision for hummocks and hollows. This trend can be explained by the fact that increasing the threshold eventually classifies all pixels as lawns, resulting in high lawn precision but sacrificing precision for other classes. The analysis also identified an optimal fill threshold of 5 cm and 4 cm for 30 cm and 50 cm DEMs, respectively that optimizes the equal error rate (intersection of precision and recall curves). The precision and recall at the equal error rate of hollows for the 30 cm DEM is also low (∼0.5) compared to other classes for the same DEM resolution (> 0.75), and for all classes of the 50 cm DEM (> 0.8).

The use of different UAV-based DEM resolutions (3 cm to 1 m) and varying fill thresholds revealed a decreasing optimal fill threshold with increasing DEM resolution (Fig. 6). The highest Kappa of all occurs at a fill threshold of 2 cm and a DEM resolution of 0.7 m. when the overall accuracy is used instead of Kappa (Figure A.1), the highest accuracy occurs at a DEM resolution of 40 cm.

3.2. Model performance and validation

3.2.1. Microforms

The robust performance of the HuHoLa microtopography classification is illustrated by the overall good F1-scores, accuracy and Kappa both for the 50 cm resolution DEM with a 4 cm threshold (Table 1), but also for the 30 cm resolution DEM (Table A.1). Overall, the 50 cm DEM appears to provide a better performance than the 30 cm DEM, with higher and more comparable precision and recall for each class in the 50 cm DEM classification (0.96 vs. 0.97 for lawns, 0.87 vs. 0.8 for hollows and 0.82 vs. 0.86 for hummocks), hence resulting in higher Kappa statistic than in the 30 cm DEM-based microtopography classification. A low recall was observed for hollows (Table A.1), resulting also in a lower hollows' F1-score with the 30 cm DEM.

3.2.2. Depth and height of hollows and hummocks as a proxy for WTD and Ts

The filled depth and height of hollows and hummocks with fix flats (HHDH with "fix flats", i.e. WTD proxy, Fig. 2 and Eq. (2)), were plotted against average field WTD measurements taken in 2022 at four locations at each of the four sites, representing different microtopographic features. The results suggest a linear relationship between measurements (non-significant at one of the sites) and this intermediary result of HuHoLa, making it a potential proxy for WTD (Fig. 7). The range of values of the WTD proxy depended on the microtopography of the area, but also on surrounding areas of the mire, as higher values were noted at Degerö Stormyr compared to the other sites. This proxy can therefore only be used after calibration using field measurements of actual WTD from each site separately. Moreover, the precision of the WTD proxy depended on the DEM resolution, and in this test, the 30 cm resolution

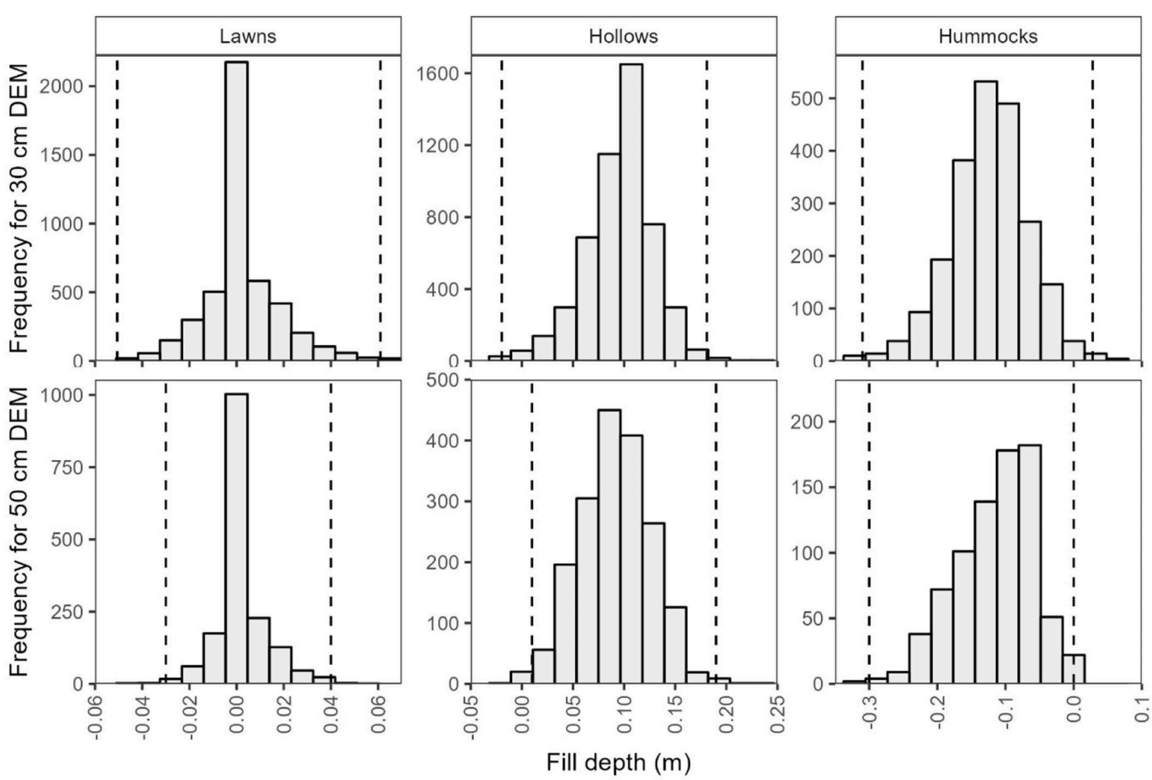

Fig. 4. Histogram of fill depth per class, for small polygons considered purely as lawns (left panels), hollows (middle panels), and hummocks (right panels). Negative and positive fill depths are fill depths in the DEM and inverted DEM, respectively. Top panels represent frequency distribution with a 30 cm DEM resolution and bottom panels represent frequency distribution with a 50 cm DEM resolution. The vertical dashed lines represent the 99% percentiles of the fill depth per class.

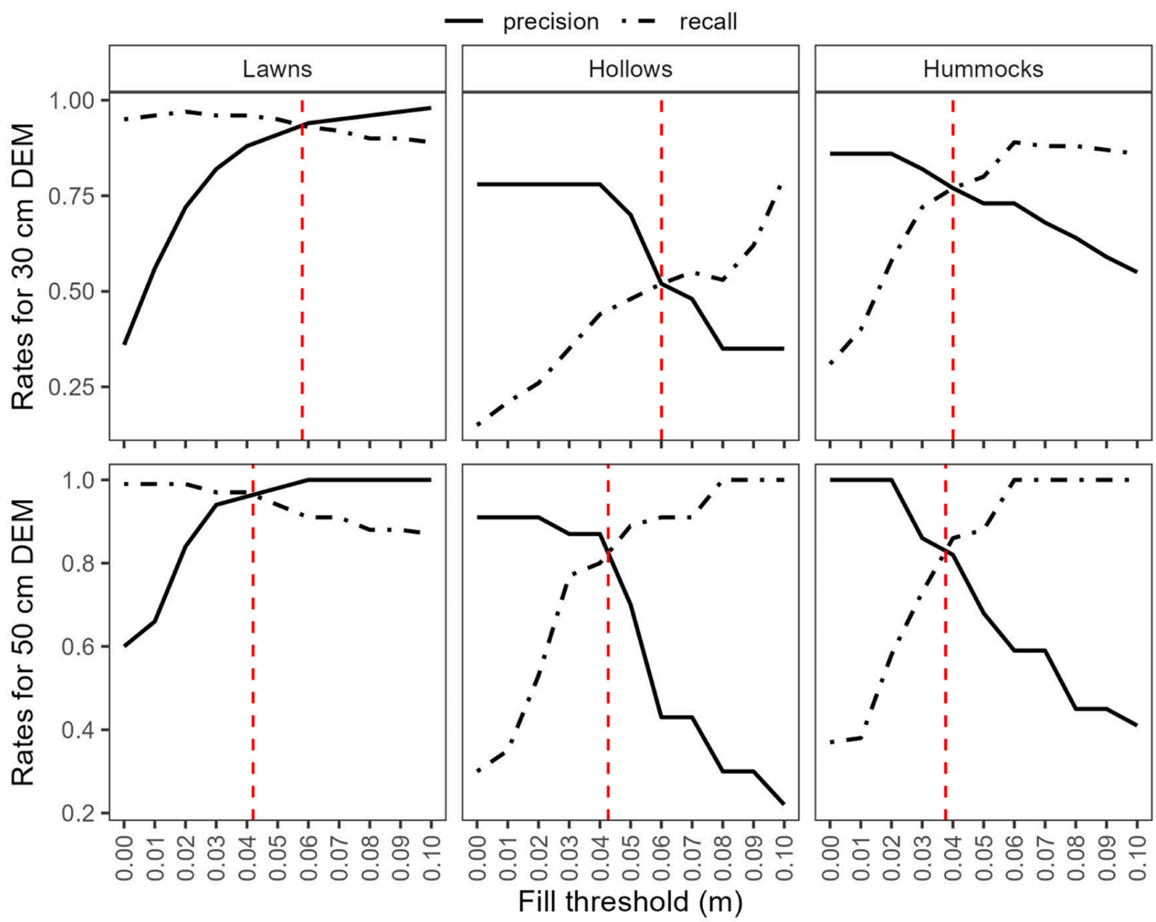

Fig. 5. Precision and recall of the different microtopography classes, from 30 cm DEM (top panels) and 50 cm DEM (bottom panels), at different fill thresholds from 0 to 10 cm. The vertical red lines represent the equal error rate, i.e. the intersection of precision and recall.

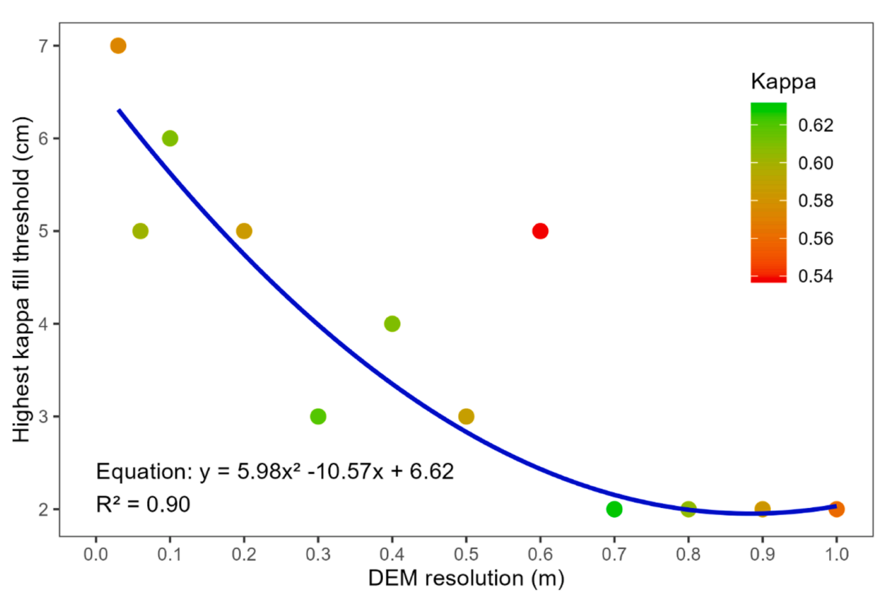

Fig. 6. Fill threshold yielding best Kappa coefficient at different DEM resolutions (3 cm, 6 cm, and 10 to 100 cm every 10 cm). The colours of the dots represent the strength of the Kappa coefficient, and the blue line is a quadratic fitted regression line.

DEM resulted in significant linear relationship WTD ~ WTD proxy (Fig. 7), while the 50 cm DEM resulted in only one site showing a significant linear relationship WTD ~ WTD proxy (Figure A.2).

Similarly, the HHDH derived from the 30 cm resolution DEM was plotted against average Ts at 10 cm depth, revealing a significant positive correlation (Fig. 8). Since HHDH is independent of the surrounding area (unlike the WTD proxy), data from all sites were combined in this linear regression. A similar significant relationship was observed when

Table 1
Performance measures for the 50 cm resolution and 4 cm fill threshold.

Class	Precision	Recall	F1-score	Support
Lawn	0.96	0.97	0.97	214
Hollow	0.87	0.80	0.83	25
Hummock	0.82	0.86	0.84	21
Accuracy			**0.94**	**260**
Kappa			0.81	260
Weighted avg.	0.88	0.87	0.88	260
Macro avg.	0.94	0.94	0.94	260

using the 50 cm resolution DEM-derived HHDH in relation to the measured Ts (Figure A.3).

3.3. HuHoLa microtopography classes map

The microtopography of Degerö Stormyr mapped using HuHoLa with a 50 cm DEM and a fill threshold of 4 cm is presented in Fig. 9. At the strings and flarks (microtopographic features in Fig. 9, circle A), lawns appear also at the transition between hummocks and hollows. Five circular plots of 50 m diameter were chosen to illustrate the different microtopographic features and the classification output from HuHoLa (Fig. 10). Additionally, two 500 m transects showing microtopography along and perpendicular to elevation gradients in a string-flark patterned area are presented in Figure A.8. Overall similar results were obtained using the 30 cm DEM for the classification (Figures A.4, A.5 and A.7). The five-class microtopography map is also presented in Figure A.6.

4. Discussion

4.1. HuHoLa – an advanced model for classification of peatland microtopography

Accurate classification of peatland microtopography is essential for improving our understanding of these ecosystems, particularly regarding their hydrological and biogeochemical functions. Traditional models have employed various methodologies, often based on sophisticated algorithms (e.g., Graham et al., 2020) or requiring extensive field data (e.g., Korpela et al., 2020), but also difficult to scale over entire mires or regional scales. The HuHoLa model presents a novel simplified approach by relying solely on a digital elevation model (DEM) to classify peatland microtopography into multiple classes. This model thus advances from the binary classification (hummock-hollow) limitation of most previous methods (Brubaker et al., 2013; Graham et al., 2020; Kalacska et al., 2021; Lovitt et al., 2017; Moore et al., 2019; Stovall et al., 2019). Furthermore, its simplicity as well as its hydrological algorithm represent an advantage over the few other attempts to classify microtopography into multiple classes, which are rooted in machine learning (e.g., Korpela et al., 2020), hence requiring extensive and site-specific training features to apply at larger scales.

Peatland surface microtopography should not be confined to the traditional binary classification of hummocks and hollows, as it represents a continuous surface elevation change. The definitions of different microtopography structures are typically based on their relative positions to the average WTD, with hummocks (20 to 50 cm above the average WTD), lawns (5 to 20 cm above the average WTD) and hollows (generally below the WTD) (Rydin and Jeglum, 2013). Some transitions

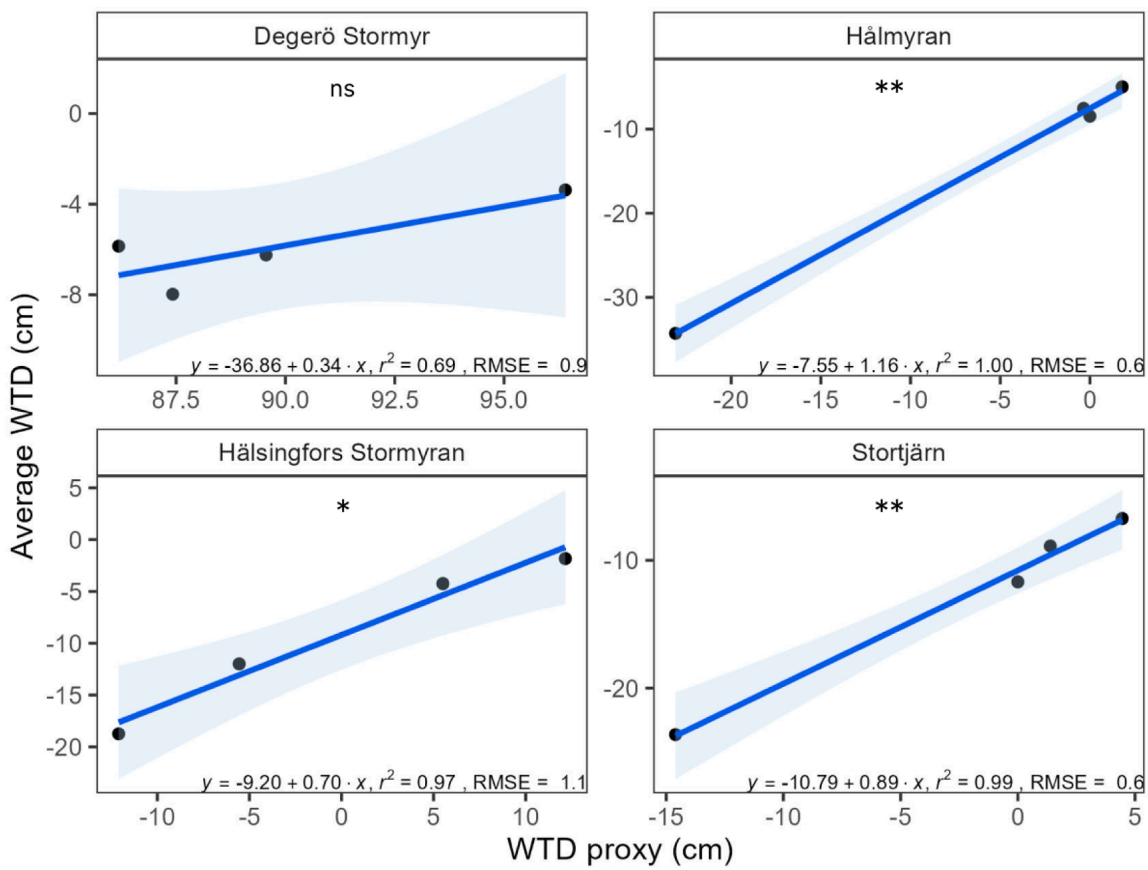

Fig. 7. Correlation between measured average water table depth (WTD) and WTD proxy from the HuHoLa model using a 30 cm resolution DEM. Each panel represents a different mire site in the mire complex. Shaded light-blue areas represent 95% confidence intervals for the linear regressions, indicating the uncertainty in the fitted relationships. The WTD proxy is the filled hollow-hummock-depth-height (Eq. (2)) in HuHoLa when a “fix flats” is applied. The * (p-value < 0.05) and ** (p-value < 0.01) represent the p-value significance of the linear relationships, while ‘ns’ means no significant linear relationship.

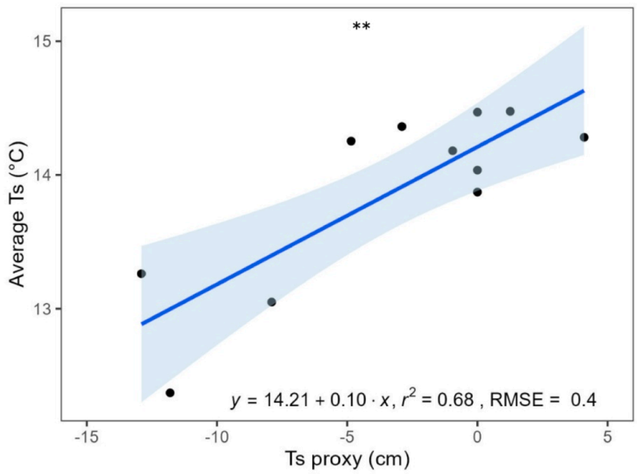

Fig. 8. Correlation between measured average soil temperature (Ts) at 10 cm depth and Ts proxy (i.e. the filled depth and height of hollows and hummocks or HHDH, Eq. (2) of the HuHoLa model) using a 30 cm resolution DEM. The shaded light-blue area represents the 95% confidence interval for the linear regression, indicating the uncertainty in the fitted relationship. No distinction was made between sites as HHDH is independent of site surroundings when no "fix flats" is applied. The ** indicates statistical significance (p-value < 0.01) for the linear relationship.

between the microtopography structures are therefore difficult to categorize, especially in a binary hummock-hollow classification. The hollow index proposed in a plot-scale study by Graham et al. (2020) is somewhat similar to the "hollow-hummock-depth-height" in HuHoLa, and is a good way to represent this microtopography continuum. When categorizing microtopography into classes, the introduction of intermediate classes (e.g. low lawns or high lawns, Korpela et al., 2020) gives a more realistic classification, with a smoother transition between the main classes. HuHoLa offers the possibility for a five-class classification, including upper level and lower level lawns intermediary classes in addition to the hummock-hollow-lawn classes. Although the five classes microtopography was not empirically validated in this study, this option to extend the model from three to five classes provides a framework for microtopographic transitions that can be useful in some other model applications.

One potential limitation of our model is that the DEM quality and precision can be influenced by different factors such as the acquisition method (e.g., LiDAR vs. SfM-derived) (Kalacska et al., 2021), peat surface oscillation, i.e. shrinking and swelling (Hrysiewicz et al., 2024; Nijp et al., 2019), vegetation height (Zhao et al., 2018), etc. While this dynamic could influence DEM-based classifications, our approach using relative elevation differences rather than absolute heights would mitigate these issues. Nonetheless, a special attention must be given to DEM acquisition (time of acquisition, atmospheric conditions, etc.) to ensure the best quality elevation data as input to the model.

While validation of the microtopography classification was limited to a single site (Degerö Stormyr) due to the availability of boardwalk infrastructure for more accessible observation, this site showcases diverse microtopography features (hummocks, lawns, hollows, strings, and flarks), demonstrating the representativeness and broader applicability of the HuHoLa method. Furthermore, the additional proxies for WTD and Ts provided by HuHoLa offer a significant advantage over other methods which are limited to microtopography classification alone.

4.2. Threshold sensitivity and DEM resolution effects on HuHoLa performance

The classification process is based on a threshold, acknowledging that lawns are not entirely flat but exhibit minor variations in elevation. Introducing this threshold allows for a more accurate representation of the three microtopography classes (hummocks, hollows and lawns), which is a significant improvement over models that overlook such nuances.

The selection of the threshold in HuHoLa is crucial, as it determines the classification outcome, but the model's sensitivity to this parameter has been rigorously evaluated using DEMs of different resolutions. This analysis does not prescribe the optimal DEM resolution for classifying

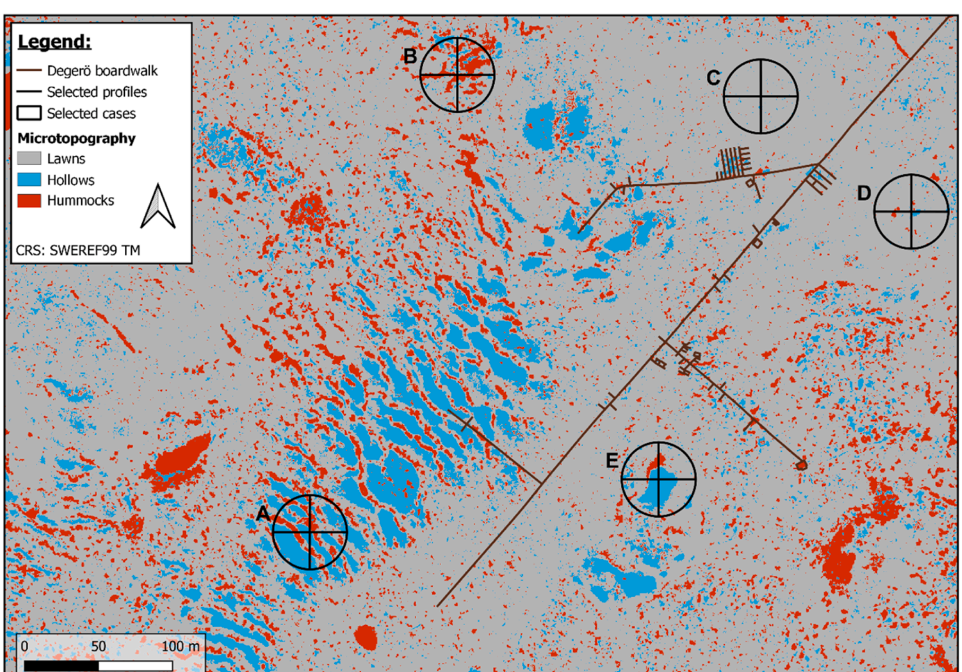

Fig. 9. Microtopography map showing the mapped microtopography using HuHoLa model with a 50 cm resolution DEM and a 4 cm threshold. The circles and vertical/horizontal cross lines represent selected cases for showing a closer view of the mapped microtopography and elevations.

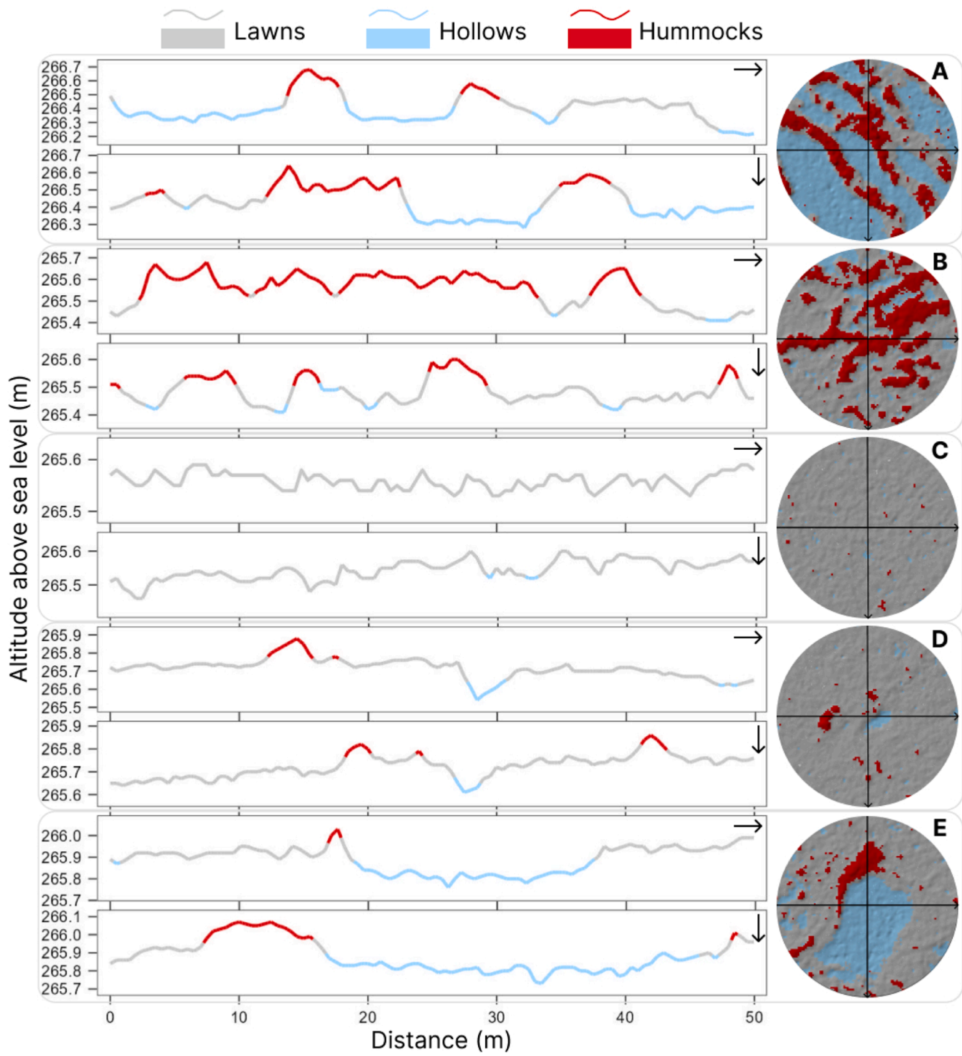

Fig. 10. Elevation profiles of a few locations in the microtopography map. The fill threshold is 4 cm, for a DEM resolution of 50 cm. The locations were chosen to represent different microforms: (A) Strings and flarks; (B) hummocks and lawns; (C) Lawns; (D) and (E) hummocks, hollows and lawns. At each location, a horizontal (left to right) and a vertical (top to bottom) arrow indicate the orientation of the elevation profiles. The Y axis graduation is variable, and a spaced Y axis as in panel C indicates little amplitude in the elevation fluctuation at the lawn.

microtopography using HuHoLa, but it suggests what threshold should be chosen according to the DEM resolution. While different thresholds for hummocks and hollows could be explored, this would add significant complexity to the model's parameterization and validation process, potentially compromising its current advantage of simplicity. The model classification performance (Kappa = 0.62 and overall accuracy = 0.88 with the 30 cm DEM, Kappa = 0.81 and overall accuracy = 0.94 with the 50 cm DEM) outperformed previous models (Kappa < 0.5 and overall accuracy < 0.8 with 10 to 25 cm DEMs; Graham et al., 2020; Stovall et al., 2019) and was comparable to a previous study where machine learning methods were applied to classify peatland microtopography (Kappa = 0.64 with a 20 cm DEM; Korpela et al., 2020). Thus, HuHoLa provides a robust classification approach that depends only on DEM characteristics, avoiding potential variability that can arise from the need for extensive site-specific training data and observer-based validation as often the case in machine learning approaches (Korpela et al., 2020).

The performance of HuHoLa is significantly influenced by the resolution of the DEM used. Our analysis demonstrated that finer DEM resolutions capture more surface rugosity, leading to a more fragmented depiction of microtopography. This increased detail can complicate the classification process, as evidenced by the lower equal error rate of hollows observed with the 30 cm resolution DEM, compared to that observed with the 50 cm resolution DEM. Additionally, artificial structures such as boardwalks can act as dams, potentially skewing the representativeness of the WTD proxy. Despite these challenges, HuHoLa exhibited robustness across various DEM resolutions, though applications to higher resolutions (< 30 cm) require further attention or validation when possible, to ensure that the resulting fragmentation is as expected in the field.

4.3. Potential applications in peatland research

The potential applications of the HuHoLa model are extensive, particularly in peatland research. By providing a fast, reliable and straightforward method for classifying microtopography, HuHoLa facilitates the scaling of plot-scale flux data to mire-ecosystem scales. Microtopographic variations strongly influence peatland greenhouse gas dynamics through their effects on hydrology, vegetation patterns, and Ts gradients, which in turn control key biogeochemical processes. The model can thus be integrated into land surface models that require microtopography parameters to simulate peatland carbon and greenhouse gas flux dynamics (Graham et al., 2022).

The secondary Ts and WTD proxy products generated by HuHoLa offer a valuable tool for spatializing the WTD and Ts in mires. Our findings indicated that WTD proxy derived from the 30 cm resolution DEM was significantly correlated with average annual field WTD observations at three out of four sites, whereas the 50 cm resolution DEM showed significant relationships at only one site. This suggests that further validation with more spatially dispersed WTD measurements and different DEM resolutions would enhance the reliability and broader applicability of the WTD proxy. On the other hand, Ts was significantly correlated with the height and depth of hollows and hummocks when no “fix flats” was applied, both with the 30 cm and the 50 cm resolution DEMs. Unlike for WTD which needed to be calibrated for each site separately, Ts can be calibrated across large mire complexes with a single linear regression. The ability to predict these key variables across peatland landscapes is particularly valuable for understanding ecosystem processes, as WTD regulates methane production and oxidation dynamics while Ts controls microbial activity and decomposition rates that drive greenhouse gas production.

While HuHoLa effectively captures peatland microtopography patterns, we acknowledge limitations and opportunities for future development. First, although the depression-filling algorithms inherently consider hydrological connectivity, our approach does not yet explicitly analyse spatial relationships between different microtopographic features in the context of water flow paths. Future studies could explore the possibility of identifying more complex patterns, such as string-flark arrangements, and how different microtopographic configurations function as ecological networks (Rinaldo et al., 2018). Such analyses could potentially derive information about hydrological connectivity, nutrient cycling, and vegetation distribution that would be valuable for integration into broader peatland ecosystem models. Second, our sensitivity analysis focused on DEM resolution effects, but more comprehensive uncertainty quantification could be conducted using global sensitivity analysis approaches (Pianosi et al., 2016) to better understand how multiple interacting factors affect classification outcomes. Furthermore, temporal dynamics of microtopography could be investigated by applying HuHoLa to time-series DEMs, potentially revealing how peatland surface patterns respond to seasonal hydrological fluctuations and longer-term environmental changes, which could contribute to understanding potential state transitions in these ecosystems.

In summary, the HuHoLa model represents a significant advancement in peatland microtopography classification. Its simplicity, robustness, and practical applications make it a valuable tool for improving our understanding of peatland processes. The additional intermediate lawn class presents a major advantage over traditional methods, in that the microtopography classification output from HuHoLa represents more realistically the peatland surface microtopography. While high-resolution DEM data ($\leq$ 1 m) is required for accurate microtopography classification, this limitation is inherent to capturing fine-scale peatland surface variations rather than specific to HuHoLa. Such datasets are becoming increasingly available through LiDAR and UAV surveys of peatland systems (Porter et al., 2018; Räsänen and Virtanen, 2019). Due to the model’s reliance on fundamental hydrological principles of surface flow and relative elevation differences, rather than site-specific characteristics or training data, it is generalizable across different peatland systems. This was demonstrated at our study site which contained diverse microform types including hummocks, hollows, lawns, strings and flarks features characteristic of many northern peatlands. The successful application across this range of microforms positions HuHoLa as a reliable tool for microtopography classification in large-scale peatland studies.

5. Conclusion

This study developed and validated the HuHoLa model, a simple and scalable DEM-based approach for classifying peatland microtopography. The model performed well at both 50 cm and 30 cm resolutions, with a threshold analysis that revealed key insights into the properties of mire microtopography, such as lawns not being entirely flat and having some small elevation fluctuations. HuHoLa’s classification of microtopography into three or five classes offers a more nuanced and realistic depiction of peatland surface structure compared to traditional binary hummock-hollow approaches. Additionally, the secondary Ts and WTD proxy outputs of HuHoLa provide a valuable tool for spatializing WTD in mires. Overall, HuHoLa represents a promising tool for large-scale peatland research, with potential applications in land surface models.

CRediT authorship contribution statement

Koffi Dodji Noumonvi: Writing – original draft, Visualization, Validation, Software, Project administration, Methodology, Formal analysis, Conceptualization. **Nils Helge Havertz:** Writing – original draft, Visualization, Validation, Methodology, Formal analysis. **Jonas Bohlin:** Writing – review & editing, Supervision, Resources, Methodology. **Sebastian van der Linden:** Writing – review & editing, Supervision. **Mats B. Nilsson:** Writing – review & editing, Supervision, Funding acquisition. **Matthias Peichl:** Writing – review & editing, Supervision, Methodology, Funding acquisition.

Declaration of competing interest

The authors declare that they have no known competing financial interests or personal relationships that could have appeared to influence the work reported in this paper.

Acknowledgements

This study was funded by the Swedish Research Council (VR, grant no 2018–03966). The Kulbäcksliden Research Infrastructure (KRI) contributes to the Swedish Infrastructure for Ecosystem Science (SITES) and the site Degerö Stormyr is part of the Swedish Integrated Carbon Observation System (ICOS-Sweden) Research Infrastructure. Financial support from the Swedish Research Council and contributing research institutes to both SITES and ICOS-Sweden are acknowledged. Support from the European Union via Erasmus mobility funding to N.H.H. is acknowledged. The authors thank the engineers of the SLU Unit for Field-based Forest research for their valuable assistance with data collection at the KRI.

Supplementary materials

Supplementary material associated with this article can be found, in the online version, at doi:10.1016/j.ecolmodel.2025.111212.

Data availability

A sample of the data used to develop the model is available along with the python script at https://github.com/bravemaster3/huhola for testing. The full datasets including the UAV images can be provided upon request.

References

Belyea, L.R., Baird, A.J., 2006. Beyond “the limits to peat bog growth”: cross-scale feedback in peatland development. Ecol. Monogr. 76, 299–322. https://doi.org/10.1890/0012-9615(2006)076 [0299:BTLTPB]2.0.CO;2.

Brubaker, K.M., Myers, W.L., Drohan, P.J., Miller, D.A., Boyer, E.W., 2013. The use of LiDAR terrain data in characterizing surface roughness and microtopography. Appl. Environ. Soil Sci. 2013, 1–13. https://doi.org/10.1155/2013/891534.

Cohen, J., 1960. A coefficient of agreement for nominal scales. Educ. Psychol. Meas. 20, 37–46. https://doi.org/10.1177/001316446002000104.

Frolking, S., Talbot, J., Jones, M.C., Treat, C.C., Kauffman, J.B., Tuittila, E.-S., Roulet, N., 2011. Peatlands in the Earth’s 21st century climate system. Environ. Rev. 19, 371–396. https://doi.org/10.1139/a11-014.

Graham, J.D., Glenn, N.F., Spaete, L.P., Hanson, P.J., 2020. Characterizing peatland microtopography using gradient and microform-based approaches. Ecosystems 23, 1464–1480. https://doi.org/10.1007/s10021-020-00481-z.

Graham, J.D., Ricciuto, D.M., Glenn, N.F., Hanson, P.J., 2022. Incorporating microtopography in a land surface model and quantifying the effect on the carbon cycle. J. Adv. Model. Earth Syst. 14. https://doi.org/10.1029/2021MS002721 e2021MS002721.

Hanczar, B., Nadif, M., 2019. Controlling and visualizing the precision-recall tradeoff for external performance indices. In: Berlingerio, M., Bonchi, F., Gärtner, T., Hurley, N., Ifrim, G. (Eds.), Machine Learning and Knowledge Discovery in Databases, Lecture Notes in Computer Science. Springer International Publishing, Cham, pp. 687–702. https://doi.org/10.1007/978-3-030-10925-7_42.

Hrysiewicz, A., Williamson, J., Evans, C.D., Jovani-Sancho, A.J., Callaghan, N., Lyons, J., White, J., Kowalska, J., Menichino, N., Holohan, E.P., 2024. Estimation and validation of InSAR-derived surface displacements at temperate raised peatlands. Remote Sens. Environ. 311, 114232. https://doi.org/10.1016/j.rse.2024.114232.

Jenson, S.K., Domingue, J.O., 1988. Extracting topographic structure from digital elevation data for geographic information system analysis. Photogramm. Eng. Remote Sens. 54, 1593–1600.

Joosten, H., Clarke, D., 2002. Wise Use of Mires and Peatlands: Background and Principles Including a Framework for Decision-making. International Mire Conservation Group.

Kalacska, M., Arroyo-Mora, J.P., Lucanus, O., 2021. Comparing UAS LiDAR and structure-from-motion photogrammetry for peatland mapping and Virtual reality (VR) visualization. Drones 5, 36. https://doi.org/10.3390/drones5020036.

Korpela, I., Haapanen, R., Korrensalo, A., Tuittila, E.-S., Vesala, T., 2020. Fine-resolution mapping of microforms of a boreal bog using aerial images and waveform-recording LiDAR. Mires Peat 26, 1–24. https://doi.org/10.19189/MaP.2018.OMB.388.

Laitinen, J., Rehell, S., Huttunen, A., 2005. Vegetation-related hydrotopographic and hydrologic classification for aapa mires (Hirvisuo, Finland). Ann. Bot. Fenn. 42, 107–121.

Lindsay, J.B., 2016. Whitebox GAT: a case study in geomorphometric analysis. Comput. Geosci. 95, 75–84. https://doi.org/10.1016/j.cageo.2016.07.003.

Lovitt, J., Rahman, M., McDermid, G., 2017. Assessing the value of UAV photogrammetry for characterizing terrain in complex peatlands. Remote Sens 715. https://doi.org/10.3390/rs9070715, 9.

Moore, P.A., Lukenbach, M.C., Thompson, D.K., Kettridge, N., Granath, G., Waddington, J.M., 2019. Assessing the peatland hummock–hollow classification framework using high-resolution elevation models: implications for appropriate complexity ecosystem modeling. Biogeosciences 16, 3491–3506. https://doi.org/10.5194/bg-16-3491-2019.

Moore, T.R., Knowles, R., 1989. The influence of water table levels on methane and carbon dioxide emissions from peatland soils. Can. J. Soil Sci. 69, 33–38. https://doi.org/10.4141/cjss89-004.

Nijp, J.J., Metselaar, K., Limpens, J., Bartholomeus, H.M., Nilsson, M.B., Berendse, F., van der Zee, S.E.A.T.M., 2019. High-resolution peat volume change in a northern peatland: spatial variability, main drivers, and impact on ecohydrology. Ecohydrology 12, e2114. https://doi.org/10.1002/ECO.2114.

Nilsson, M.B., 2002. Mire ecosystems. Encyclopedia of Life Sciences. Wiley. https://doi.org/10.1038/npg.els.0003194.

Noumonvi, K.D., Ågren, A.M., Ratcliffe, J.L., Öquist, M.G., Ericson, L., Tong, C.H.M., Järveoja, J., Zhu, W., Osterwalder, S., Peng, H., Erefur, C., Bishop, K., Laudon, H., Nilsson, M.B., Peichl, M., 2023. The Kulbäcksliden Research Infrastructure: a unique setting for northern peatland studies. Front. Earth Sci. 11, 1194749. https://doi.org/10.3389/feart.2023.1194749.

Nungesser, M.K., 2003. Modelling microtopography in boreal peatlands: hummocks and hollows. Ecol. Model. 165, 175–207. https://doi.org/10.1016/S0304-3800(03)00067-X.

Page, S.E., Baird, A.J., 2016. Peatlands and Global change: response and resilience. Annu. Rev. Environ. Resour. 41, 35–57. https://doi.org/10.1146/annurev-environ-110615-085520.

Pianosi, F., Beven, K., Freer, J., Hall, J.W., Rougier, J., Stephenson, D.B., Wagener, T., 2016. Sensitivity analysis of environmental models: a systematic review with practical workflow. Environ. Model. Softw. 79, 214–232. https://doi.org/10.1016/j.envsoft.2016.02.008.

Planchon, O., Darboux, F., 2002. A fast, simple and versatile algorithm to fill the depressions of digital elevation models. CATENA 46, 159–176. https://doi.org/10.1016/S0341-8162(01)00164-3.

Porter, C., Morin, P., Howat, I., Noh, M.-J., Bates, B., Peterman, K., Keesey, S., Schlenk, M., Gardiner, J., Tomko, K., Willis, M., Kelleher, C., Cloutier, M., Husby, E., Foga, S., Nakamura, H., Platson, M., Wethington, M., Williamson, C., Bauer, G., Enos, J., Arnold, G., Kramer, W., Becker, P., Doshi, A., D'Souza, C., Cummens, P., Laurier, F., Bojesen, M., 2018. ArcticDEM, Version 3. https://doi.org/10.7910/DVN/OHHUKH.

Pouliot, R., Rochefort, L., Karofeld, E., 2011. Initiation of microtopography in revegetated cutover peatlands: initiation of microtopography. Appl. Veg. Sci. 14, 158–171. https://doi.org/10.1111/j.1654-109X.2010.01118.x.

Räsänen, A., Virtanen, T., 2019. Data and resolution requirements in mapping vegetation in spatially heterogeneous landscapes. Remote Sens. Environ. 230, 111207. https://doi.org/10.1016/j.rse.2019.05.026.

Rinaldo, A., Gatto, M., Rodriguez-Iturbe, I., 2018. River networks as ecological corridors: a coherent ecohydrological perspective. Adv. Water Resour. 112, 27–58. https://doi.org/10.1016/j.advwatres.2017.10.005.

Rydin, H., Jeglum, J.K., 2013. The Biology of Peatlands. Oxford University Press. https://doi.org/10.1093/acprof:osobl/9780199602995.001.0001.

Rydin, H., Jeglum, J.K., 2006. Hydrology of peatlands. In: Rydin, Hakan, Jeglum, J.K. (Eds.), The Biology of Peatlands. Oxford University Press, p. 0. https://doi.org/10.1093/acprof:oso/9780198528722.003.0008.

Sim, J., Wright, C.C., 2005. The Kappa Statistic in Reliability Studies: use, interpretation, and sample size requirements. Phys. Ther. 85, 257–268. https://doi.org/10.1093/ptj/85.3.257.

Sirin, A.A., 2023. Mires and peatlands: carbon, greenhouse gases, and climate change. Biol. Bull. Rev. 12, S123–S139. https://doi.org/10.1134/S2079086422080096.

Stovall, A.E.L., Diamond, J.S., Slesak, R.A., McLaughlin, D.L., Shugart, H., 2019. Quantifying wetland microtopography with terrestrial laser scanning. Remote Sens. Environ. 232, 111271. https://doi.org/10.1016/j.rse.2019.111271.

Wang, L., Liu, H., 2006. An efficient method for identifying and filling surface depressions in digital elevation models for hydrologic analysis and modelling. Int. J. Geogr. Inf. Sci. 20, 193–213. https://doi.org/10.1080/13658810500433453.

Wu, Y., Blodau, C., 2013. PEATBOG: a biogeochemical model for analyzing coupled carbon and nitrogen dynamics in northern peatlands. Geosci. Model Dev. 6, 1173–1207. https://doi.org/10.5194/gmd-6-1173-2013.

Zhao, B., Zhuang, Q., 2023. Peatlands and their carbon dynamics in northern high latitudes from 1990 to 2300: a process-based biogeochemistry model analysis. Biogeosciences 20, 251–270. https://doi.org/10.5194/bg-20-251-2023.

Zhao, X., Su, Y., Hu, T., Chen, L., Gao, S., Wang, R., Jin, S., Guo, Q., 2018. A global corrected SRTM DEM product for vegetated areas. Remote Sens. Lett. 9, 393–402. https://doi.org/10.1080/2150704X.2018.1425560.